FEBS Letters 588 (2014) 4631–4636

FEBS Letters

journal homepage: www.FEBSLetters.org

Formation and dimerization of the phosphodiesterase active site of the *Pseudomonas aeruginosa* MorA, a bi-functional c-di-GMP regulator

Curtis William Phippen, Halina Mikolajek, Henry George Schlaefli, Charles William Keevil, Jeremy Stephen Webb, Ivo Tews *

Centre for Biological Sciences and Institute for Life Sciences, Life Sciences Building B85, The University of Southampton, University Rd, Southampton, Hampshire, SO17 1BJ, United Kingdom

ARTICLE INFO

Article history:
Received 14 October 2014
Revised 3 November 2014
Accepted 3 November 2014
Available online 11 November 2014

Edited by Richard Cogdell

Keywords:
Motility regulator A
Diguanylate cyclases
Phosphodiesterases
Cyclic dimeric guanosine monophosphate
Biofilm dispersal

ABSTRACT

Diguanylate cyclases (DGC) and phosphodiesterases (PDE), respectively synthesise and hydrolyse the secondary messenger cyclic dimeric GMP (c-di-GMP), and both activities are often found in a single protein. Intracellular c-di-GMP levels in turn regulate bacterial motility, virulence and biofilm formation. We report the first structure of a tandem DGC–PDE fragment, in which the catalytic domains are shown to be active. Two phosphodiesterase states are distinguished by active site formation. The structures, in the presence or absence of c-di-GMP, suggest that dimerisation and binding pocket formation are linked, with dimerisation being required for catalytic activity. An understanding of PDE activation is important, as biofilm dispersal *via* c-di-GMP hydrolysis has therapeutic effects on chronic infections.

1. Introduction

Biofilms are the major form of bacterial organisation and are a common problem in chronic infections [1,2]. For the bacterium *Pseudomonas aeruginosa*, chronic infection and biofilm formation is the main cause of mortality for sufferers of cystic fibrosis [3]. Biofilms display an increased persistence and tolerance to antibiotics [4]. Physiologically, biofilm formation is associated with high levels of the secondary messenger cyclic dimeric guanosine monophosphate (c-di-GMP) [5,6], which is synthesised by diguanylate cyclases (DGC) from two guanosine triphosphate (GTP) molecules [7]. Reduction in c-di-GMP levels can be achieved by NO stimulation, leading to biofilm dispersal, thereby offering new strategies to treat biofilm-associated infection [8,9].

Biofilm dispersion is linked to c-di-GMP hydrolysis by two types of phosphodiesterases (PDE) [10] with either an EAL [11] or a HD-GYP [12] motif. The two classes differ with respect to their hydrolysis products. HD-GYP domains hydrolyse c-di-GMP into two GMP molecules and have been shown to utilise trinuclear iron binding [13]. EAL domains, however, hydrolyse c-di-GMP to the linear di-nucleotide 5′-pGpG and additionally require a dimerisation event for PDE activation [14]. EAL domains have been identified to contain two key surface helices providing a binding groove for an antiparallel dimer formation [15,16]. In addition to the EAL motif, a second conserved DDFGTG(YSS) sequence motif coordinates the Mg^{2+} ions required for activity [14]. Domains with a degenerate DDFGTG and EAL motif are catalytically inactive and instead function as c-di-GMP sensor proteins [17].

EAL phosphodiesterase domains often occur in tandem with a diguanylate cyclase domain, in a single protein [18]. A structure of these dual domain proteins is known from the DGC–PDE c-di-GMP sensor protein LapD [19]. Conversion to the sensor is explained by a lack of the conserved EAL and DDFGTG motifs required for PDE activity. The determination of the structure of LapD provides insight into the regulation of nucleotide binding, as the isolated EAL domain can bind c-di-GMP, but in the tandem domain structure the nucleotide-binding pocket is obstructed. For proteins with dual activity, the underlying question is how

Abbreviations: c-di-GMP, cyclic dimeric guanosine monophosphate; DGC, diguanylate cyclase; GTP, guanosine triphosphate; MorA, motility regulator A; PDB, protein data bank; PDE, phosphodiesterase; pGpG, phosphate guanosine phosphate guanosine

* Corresponding author.
E-mail address: Ivo.Tews@soton.ac.uk (I. Tews).

http://dx.doi.org/10.1016/j.febslet.2014.11.002
0014-5793/

the two opposing activities of cyclase and phosphodiesterase are controlled.

We have studied the tandem domain protein motility regulator A (MorA), conserved across *Pseudomonas* species [20]. Additional to PDE and DGC domains, the cytosolic segment contains four PAS sensory domains (Per-Arnt-Sim homology) [21]. The protein is localised to the membrane by two N-terminal transmembrane helices and can affect bacterial motility [20]. MorA has been linked to fimbriae and flagella formation, prerequisites for biofilm formation and dispersal, respectively [22,23]. The protein is also reported to control the timing of flagella development and regulate sensory chemotaxis pathways [20]. The C-terminal PDE domain of MorA shows intact DDFGTG and EAL motifs, indicative of phosphodiesterase activity.

Here, we report the catalytic activity and structure of the tandem DGC–PDE fragment from MorA in the absence and presence of c-di-GMP and two structures of the isolated PDE in absence of nucleotide, but distinguished by dimerisation. Our data describe two states of the PDE nucleotide-binding pocket. The four structures suggest that dimerisation is involved in the formation of the nucleotide-binding pocket and catalytic activity. Understanding of PDE activation is highly sought after as biofilm dispersal results in bacteria becoming susceptible to antibiotics.

2. Materials and methods

2.1. Molecular biology and protein purification

Genomic DNA of *P. aeruginosa* PAO1 was isolated using the DNeasy blood and tissue kit (Qiagen). MorA gene PA4601 was amplified by PCR using Phusion Polymerase (Finnzymes); PCR fragments were restriction digested and inserted into the expression vector pET-28a (Novagen). The following fragments were cloned with N-terminal fusion tags: $DGC^{978–1144}$, $PDE^{145–1409}$ and tandem DGC–$PDE^{978–1409}$. The D1310N/D1311N point mutations were introduced into tandem DGC–$PDE^{978–1409}$ using the Lightning QuikChange kit (Invitrogen).

For recombinant expression of all proteins, BL21 DE3 *Escherichia coli* competent cultures were grown in LB medium and induced by 1 mM isopropyl-beta-D-thiogalactopyranoside (Melford) at an optical density OD_{600} of 0.6. The cultures were collected after 20 h growth at 18 °C by centrifugation. Cells from 2 l cultures were resuspended in 50 ml 50 mM HEPES buffered at pH 7.5 with 300 mM NaCl, 5% glycerol, lysed by sonication, and centrifuged at 16,000 rpm for 40 min (Beckman Avanti centrifuge, JA25.50 rotor). The supernatant was loaded onto 4 ml Ni-NTA resin (Qiagen), equilibrated with buffer A (50 mM HEPES buffered at pH 7.5 with 300 mM NaCl, 2 mM $MgCl_2$, 5% glycerol, 2 mM β-mercaptoethanol and 20 mM imidazole), followed by washes with buffer A containing 80 mM imidazole and elution using buffer A containing 300 mM imidazole. Following concentration over spin concentrators (Generon), the eluate was loaded onto an S75 16/600 size exclusion column (GE) equilibrated in 50 mM HEPES buffered at pH 7.5 with 300 mM NaCl, 2 mM $MgCl_2$ and 2 mM β-mercaptoethanol. Fractions containing the desired protein, confirmed by SDS–PAGE, were pooled and concentrated using spin concentrators (Generon).

2.2. Enzymatic assay

Activity of MorA fragments was determined by an enzyme assay followed by HPLC analysis of nucleotides, adapted from [24]. Enzymes were used at a concentration of 40 μM; these were mixed with 0.1 mM GTP (Biolog) in 50 mM HEPES buffered at pH 7.5, with 300 mM NaCl, 2 mM $MgCl_2$ and 2 mM β-mercaptoethanol to 200 μl and incubated at room temperature for 1 h. Samples were then run on a combination of a C4 and a C18 RPC column (Vydac), using a Shimadzu HPLC system, in buffer A (100 mM KPO_4 buffered at pH 6) with an elution gradient of 15 min into buffer B (70% buffer A with 30% methanol). Absorbance at 254 nm was used for detection. The system was calibrated using GTP (Sigma), 5′-pGpG (Biolog) and c-di-GMP, prepared by enzymatic synthesis from GTP, using purified YdeH as described in [25].

2.3. Bis-4pNPP analysis

PDE activity was measured in 1 ml total volume containing 0.4 mg/ml protein, 5 mM bis-(*p*-nitrophenyl) phosphate (Sigma) and 50 mM Tris pH 9.2 with 5 mM $MgCl_2$ and 50 mM NaCl. The reaction was carried out at 37 °C. After 180 min the absorbance of the hydrolysed product was measured at 405 nm using a nanodrop spectrophotometer (Thermo Scientific). Controls contained heat inactivated proteins (100 °C, 5 min).

2.4. Structure determination and analysis

Purified proteins were crystallised in sitting drop 96-well plates using a Gryphon nanodrop dispenser (Art Robbins Instruments). Crystal hit optimisation was carried out using a Minstrel DT alchemist (Rigaku). Data were collected at the Southampton Diffraction Centre, the Diamond Light Source (DLS, Oxford) and the European Synchrotron Radiation Facility (ESRF, Grenoble). Data reduction, molecular replacement and refinement were carried out with CCP4 [26] and Phenix [27,28]; models were built using Coot [29] and automated water structure building in ArpWarp [30] (Table 1). Dyndom was used to determine hinge regions [31]. PISA was used to calculate protein–protein interfaces [32]. Pymol was used to create figures (Schrödinger).

DGC–$PDE^{978–1409}$ D1310N/D1311N mutant (PDB 4RNF): crystallised at 21 °C and a concentration of 26 mg/ml in 0.12 M Morpheus alcohols, 0.1 M Buffer System 1, 30% EDO P8K (Molecular Dimensions). Data were collected at DLS I03 to a resolution of 2.85 Å. The structure was solved by molecular replacement with dimeric $PDE^{1145–1409}$ (this study), and the GGDEF domain from *Methylococcus capsulatus* (PDB 3ICL, [33]).

DGC–$PDE^{978–1409}$ c-di-GMP complex (PDB 4RNH): crystallised at 21 °C and a concentration of 20 mg/ml and 2 molar excess of GTP (Sigma) in 0.2 M sodium thiocyanate, 20% w/v PEG 3350. Data were collected at DLS I04 to a resolution of 2.45 Å. The structure was solved by molecular replacement using the DGC–$PDE^{978–1409}$ D1310N/D1311N mutant (this study). Instead of GTP, we obtained c-di-GMP bound to the active site of the PDE in this crystal form.

Dimeric $PDE^{1145–1409}$ (PDB 4RNI): crystallised at 21 °C and a concentration of 10 mg/ml and 3 molar excess of 5′-pGpG (Biolog) in 0.1 M Morpheus Buffer System 3, 0.1 M amino acids, 30% GOL P4K (Molecular Dimensions). Data were collected at DLS I04 to a resolution of 2.17 Å. The structure was solved by molecular replacement, using the *Thiobacillus denitrificans* phosphodiesterase (PDB 3N3T, [34]). 5′-pGpG was not visible in the final structure but required for crystallisation.

Monomeric $PDE^{1145–1409}$ (PDB 4RNJ): crystallised at 21 °C and a concentration of 12 mg/ml in 0.1 M Morpheus Buffer System 1, 0.09 M NPS, 30% EDO P8K (Molecular Dimensions). Data were collected at ESRF ID14-1 to a resolution of 2.32 Å. The structure was solved by molecular replacement with dimeric $PDE^{1145–1409}$ (this study).

3. Results and discussion

3.1. Activity assay

To confirm that MorA is a suitable system to study bi-functional c-di-GMP regulation, we first ensured that MorA has diguanylate

Table 1
X-ray data collection and refinement statistics.

	DGC–PDE$^{978–1409}$ Mutant D1310/1311N	PDE$^{1145–1409}$ Dimer c-di-GMP complex	DGC–PDE$^{978–1409}$ Apo-Monomer	PDE$^{1145–1409}$ Apo-Dimer
Accession code	4RNF	4RNH	4RNJ	4RNI
Space group	P1	$P3_121$	$P2_12_12_1$	$P2_12_12$
Cell *a*, *b*, *c* (Å)	40.7, 47.4, 60.0	81.3, 81.3, 128.0	52.0, 79.8, 138.5	35.6, 94.5, 154.6
Angles α, β, γ (°)	82.15, 71.63, 70.66	90, 90, 120	90, 90, 90	90, 90, 90
Resolution (Å)[a]	28.46–2.85 (3.26–2.85)	61.7–2.45 (2.52–2.45)	48.75–2.32 (2.4–2.32)	77.35–2.17 (2.23–2.17)
R_{merge} (%)[a]	17.4 (59.1)	10.7 (74.6)	7.2 (67.8)	11.0 (78.8)
I/σ (I)[a]	7.4 (2.4)	14.5 (2.6)	13.87 (1.8)	18.3 (3.9)
No. unique reflections	9235	18546	25720	28764
Completeness (%)[a]	98.5 (98.0)	100 (99.5)	99.7 (98.4)	100 (99.8)
Redundancy [a]	2.8 (2.7)	8.1 (6.3)	4.28 (3.69)	13.3 (13.4)
Refinement				
R_{work}/R_{free} (%)	23.1/27.7	18.7/24.3	19.8/25.3	18.4/23.5
No. protein atoms	3332	3525	3996	3961
No. ligand atoms/ion	–	(c-di-GMP/Mg^{2+}) 68/4	–	–
No. waters	12	140	121	156
Protein B_{factor} (Å^2)	36.3	45.3	42.6	36.9
Ligand/ion B_{factor} (Å^2)	–	(c-di-GMP/Mg^{2+}) 54.2/50.4	–	–
Water B_{factor} (Å^2)	52.6	45.1	28.9	35
Bond lengths rmsd (Å)	0.014	0.006	0.013	0.002
Bond angles rmsd (°)	1.370	0.815	1.431	0.860
Ramachandran (%)				
Preferred regions	95.96	97.58	98.61	98.41
Allowed regions	3.80	2.42	1.39	1.59
Outliers	0.24	0	0	0
Closest contact	Monomer A and symmetry A (X − 1, Y + 1, Z) ΔG of −5 kJ/mol with a surface area of 1002.7 Å^2	Monomer A and symmetry A (X − Y, −Y, −Z-1/3) ΔG of −14.5 kJ/mol with a surface area of 1631.6 Å^2	Monomer A and B ΔG of −4 kJ/mol with a surface area of 776.5 Å^2	Monomer A and B ΔG of −11.6 kJ/mol with a surface area of 1070.8 Å^2

[a] Values in parentheses are for the highest-resolution bin.

cyclase and phosphodiesterase activities. Our analysis is based on RPC-HPLC separation of nucleotide products. When an isolated DGC$^{978–1144}$ fragment was incubated with GTP, a retention product at 10 minutes is observed that corresponds to the c-di-GMP standard (Fig. 1A). This indicates MorA has diguanylate cyclase activity.

To study the bi-functional enzyme, we incubated the MorA fragment containing both DGC and PDE domains (DGC–PDE$^{978–1409}$) with GTP. HPLC analysis of reaction products showed a peak with a decreased retention time, compared with c-di-GMP that corresponds to the 5′-pGpG standard (Fig. 1A). Since no c-di-GMP was added in this experiment this indicates MorA's DGC produced c-di-GMP, which we observed as a small peak, consistent with the standard. However, the majority is converted to the linear nucleotide indicating MorA also has phosphodiesterase activity. The PDE containing fragments were further tested with the generic PDE substrate bis-(*p*-nitrophenyl) phosphate (Table S1), confirming activity in the PDE domain.

To corroborate the DGC activity in the tandem DGC–PDE fragment, we mutated the PDE domain to obtain a catalytically inactive variant. To do this, the DDFGTG sequence motif was replaced with NNFGTG (D1310N and D1311N). The two aspartates that were replaced coordinate the Mg^{2+} ions required for activity [14]. HPLC analysis of reaction products after incubation with GTP showed a peak that corresponds to the c-di-GMP standard (Fig. 1A). Thus, the mutant DGC–PDE fragment retained DGC activity but was unable to produce 5′-pGpG, indicating the mutations render the PDE inactive (Table S1).

The activity assays showed that MorA's DGC and PDE domains could synthesise and hydrolyse c-di-GMP respectively. Since MorA has both, DGC and PDE catalytic activity, it is implicit that MorA should have mechanisms to control these opposing activities. Likely mechanisms are either interaction of PDE and DGC domains, or oligomerisation. Indeed, dimerisation of DGC domains is required for cyclase activity, as each monomer contributes one nucleotide to the product, and dimerisation of PDE domains is known to influence phosphodiesterase activity [15,16]. We therefore investigated the protein fragments for oligomerisation and initiated structural studies.

3.2. Nucleotide free state of MorA DGC–PDE

To determine the nucleotide free state of the tandem fragment we used the MorA DGC–PDE$^{978–1409}$ D1310 and D1311 mutant; experiments to acquire a nucleotide free structure of the wild type tandem fragment yielded non-diffracting crystals. The overall structure of MorA's DGC–PDE$^{978–1409}$ mutant is comprised of an arrangement that separates the DGC and PDE domains into an open conformation (Fig. 1B and C). A 31 Å long helix (named H helix, see Section 3.4.), involving 19 amino acid residues (A1145–L1167), links the DGC and PDE domains. The DGC of MorA adopts the archetypical GGDEF domain fold that consists of five alpha helices surrounding a five stranded beta sheet (αβααββαϖ βαβ) (Fig. 1B) [35]. The DGC is nucleotide free and the nucleotide recognising helix α2 is disordered. The conformation seen does not preclude DGC dimerisation. MorA's PDE forms the canonical $(\beta/\alpha)_8$ barrel in which the first beta strand is reversed [11], with respect to classic TIM topology (Fig. 1C) [36]. The open conformation is stabilised by direct contact between residues K1076 and E1213 located on the DGC-α4 and PDE-α4′ helices (SFig. 1). In the open conformation, both the PDE and DGC active sites are accessible.

An interesting feature of the MorA DGC–PDE$^{978–1409}$ mutant is the local structure around helix PDE-α5. The PDE-α5 helix in MorA is extended and consists of residues G1315–Q1324, resulting in the removal of the DDFGTG motif from the active site, which would be required for Mg^{2+} coordination and activity. A nucleotide free structure of the wild type PDE was determined using the isolated fragment, PDE$^{1145–1409}$. Intriguingly, this monomeric PDE$^{1145–1409}$ structure shows the same features as the MorA DGC–PDE$^{978–1409}$ mutant with an extended PDE-α5 helix in a Mg^{2+} free state and the DDFGTG motif removed from the active site (Fig. 2A). Since formation of the helix PDE-α5 extension removes catalytic

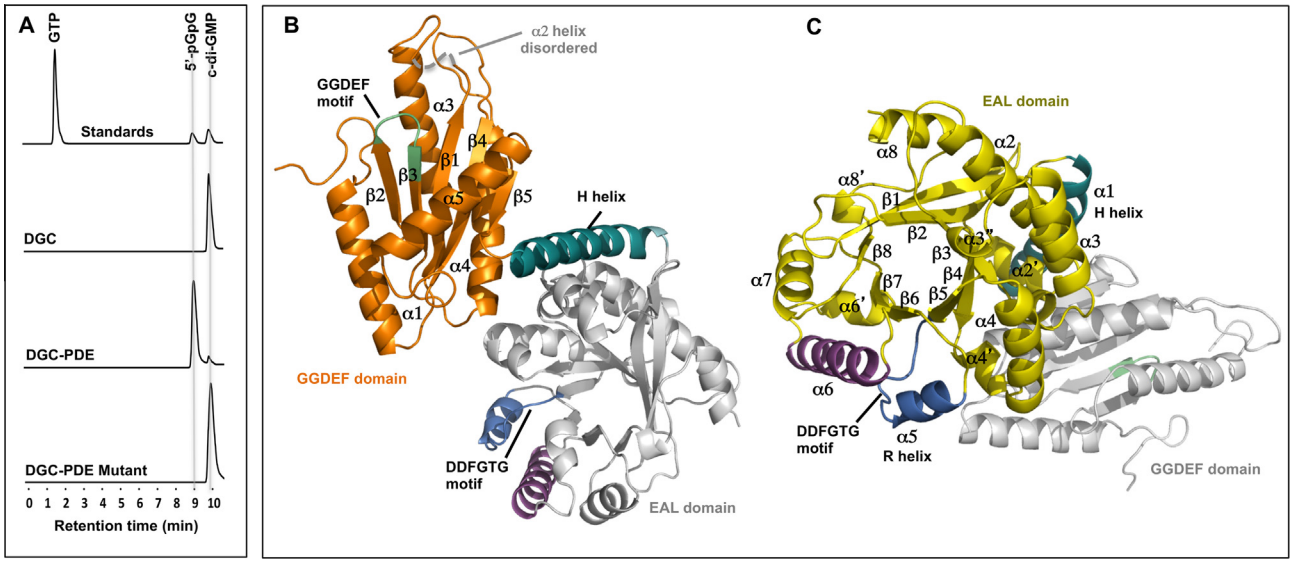

Fig. 1. Enzymatic activity and crystal structure of the nucleotide free state of MorA tandem DGC–PDE. (A) HPLC analysis of nucleotide loading states after incubation with GTP; DGC, DGC$^{978–1144}$; DGC–PDE, DGC–PDE$^{978–1409}$; DGC–PDE mutant, DGC–PDE$^{978–1409}$ D1310N/D1311N; standards as indicated; *x*-axis in minutes, *y*-axis AU at λ = 254. (B) MorA DGC–PDE$^{978–1409}$ D1310N/D1311N structure with the DGC domain in orange, the GGDEF sequence motif is highlighted in green. Alpha helices and beta sheets are labelled. The α2 helix is disordered (dashed line). The H helix (cyan) links the DGC domain to the PDE domain (grey). (C) MorA DGC–PDE$^{978–1409}$ D1310N/D1311N structure in different orientation to (B) shows the PDE domain in yellow. The active site DDFGTG motif and the α5 helix or R helix are highlighted in blue, the α6 helix is shown in purple. The H helix (cyan) links the PDE domain to the DGC domain (grey). Alpha helices and beta sheets are labelled in accordance to classical TIM barrels.

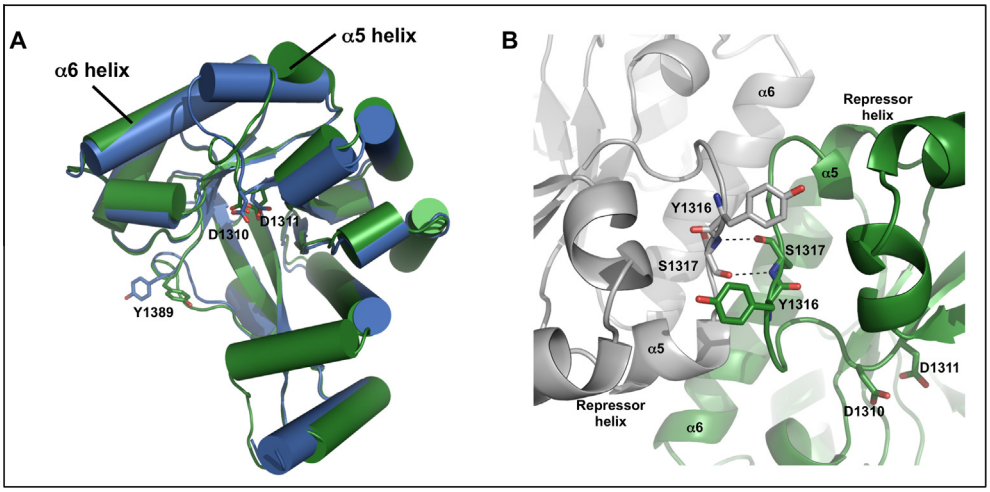

Fig. 2. MorA PDE dimer formation and conformational changes of the R helix. (A) Overlay of monomeric PDE$^{1145–1409}$ (marine blue) with the dimeric PDE$^{1145–1409}$ (green). The two structures differ in the orientation and length of the R helix (PDE-α5). The R helix is extended in the monomeric PDE structure (G1315–Q1324, marine blue) but shorter in the dimeric PDE structure (L1319–Q1324, green) resulting in different conformations of the DDFGTGYSS motif. Y1389 acts as a gate to the active site and is seen in two different side chain rotamer conformations. (B) The dimer interface is formed through reciprocal contact of Y1316 and S1317 from monomer A (green) and a symmetry molecule (−X, −Y + 1/2, Z + 1/2) (grey). These two residues are part of the DDFGTG**YS**S motif. The dimeric structure is characterised by a short R helix (α5, L1319–Q1324).

residues from the active site, we have named this helix repressor helix (R helix). It is known that dimerisation regulates PDE activity and hence we went on to characterise a structure of a PDE dimer to investigate the nature of this structural rearrangement.

3.3. PDE dimerisation influences the conformation of the R helix

To promote dimer formation, we crystallised the isolated PDE$^{1145–1409}$ domain of MorA in the presence of 5′-pGpG. Crystallisation yielded a nucleotide-free dimer with contacts around the α5-helix (R helix) and the α6 helix (Fig. 2B). PDE domain dimers have been previously identified (Table S2) [15–17,19,37,38]. PDE dimerisation involving PDE-α6 and the R helix has implications for active site formation. The PDE dimer contact between residues Y1316 and S1317 stabilises the loop formed by residues G1315–S1318 and thus stabilises a state in which the R helix is shortened (L1319–Q1324) (Fig. 2A). The shorter conformation of the R helix is consistent with the previously solved catalytically active c-di-GMP bound structure from *T. denitrificans* phosphodiesterase (PDB 3N3T). An extended R helix (G1315–Q1324), as seen in the nucleotide-free structures, is not compatible with dimer formation, as it would lead to clashes around the dimer interface and not allow residues Y1316 and S1317 of the ^{1310}DDFGTGYSS^{1318} motif to contribute to dimer formation. Conservation of the YS residues is, therefore, explained by their involvement in PDE dimerisation (Fig. 2).

Dimerisation around the R helix, therefore, stabilises the DDFGTGYSS motif into an extended loop conformation. However, no nucleotide or Mg^{2+} are present in the active site. The dimeric $PDE^{1145-1409}$ structure is presumably observed post-hydrolysis, where the product 5′-pGpG has left the binding site. To understand the significance of the different R helix conformations, we wanted to study the nucleotide-bound state of the PDE within MorA.

3.4. Nucleotide bound state of MorA DGC–PDE

To obtain the c-di-GMP complex, we had to mix the tandem $DGC–PDE^{978-1409}$ wild type fragment with excess GTP immediately before crystallisation. Binding of c-di-GMP into the native PDE active site of MorA results in PDE dimerisation of the tandem fragment (Fig. 3A). The orientation of PDE dimer is similar to the one observed within the isolated $PDE^{1145-1409}$ structure in the presence of 5′-pGpG (Fig. 2 and Table S2). The DGC domains in this dimer do not interact with one another (Fig. 3B).

In the nucleotide-bound form the R helix adopts the shorter conformation (L1319–Q1324), compared to the wild type nucleotide free monomeric PDE (G1315–Q1324) (Fig. 3C). The shorter conformation of the R helix allows the extended loop conformation of the DDFGTG motif to contribute to active site formation, where residues D1310 and D1311 of the DDFGTG motif, along with residue E1189 of the EAL motif coordinate two Mg^{2+} ions (Fig. 3C and SFig. 2). Interpretation of this c-di-GMP complex is that of a Michaelis complex that has yet to undergo activation [8], as the tandem DGC–PDE is able to hydrolyse c-di-GMP to 5′pGpG (Fig. 1A).

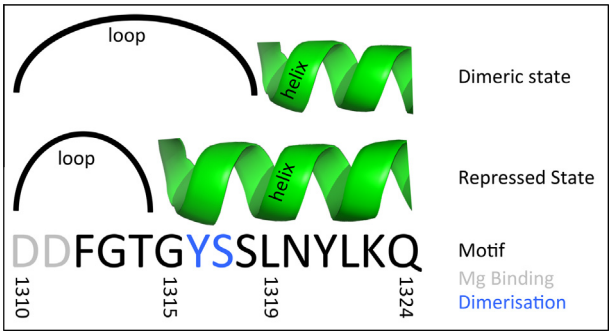

Fig. 4. The role of amino acids in the DDFGTGYSS motif. The side chains of two aspartate residues (DD) are involved in Mg^{2+} coordination and the side chains of the tyrosine/serine residues (YS) are involved in PDE dimerisation.

Comparison of the PDE domains presented here allows for an assignment of two distinct states (Figs. 3C and 4). The nucleotide-free structures show the repressed state with an incomplete active site, characterised by an extension of the R helix (PDE-α5), which removes the DDFGTG motif from the active site and results in the loss of Mg^{2+} binding. This state is different to the dimeric state of the $PDE^{1145-1409}$ and c-di-GMP bound DGC–PDE, where a shorter R helix is formed. Interactions at the dimeric interface

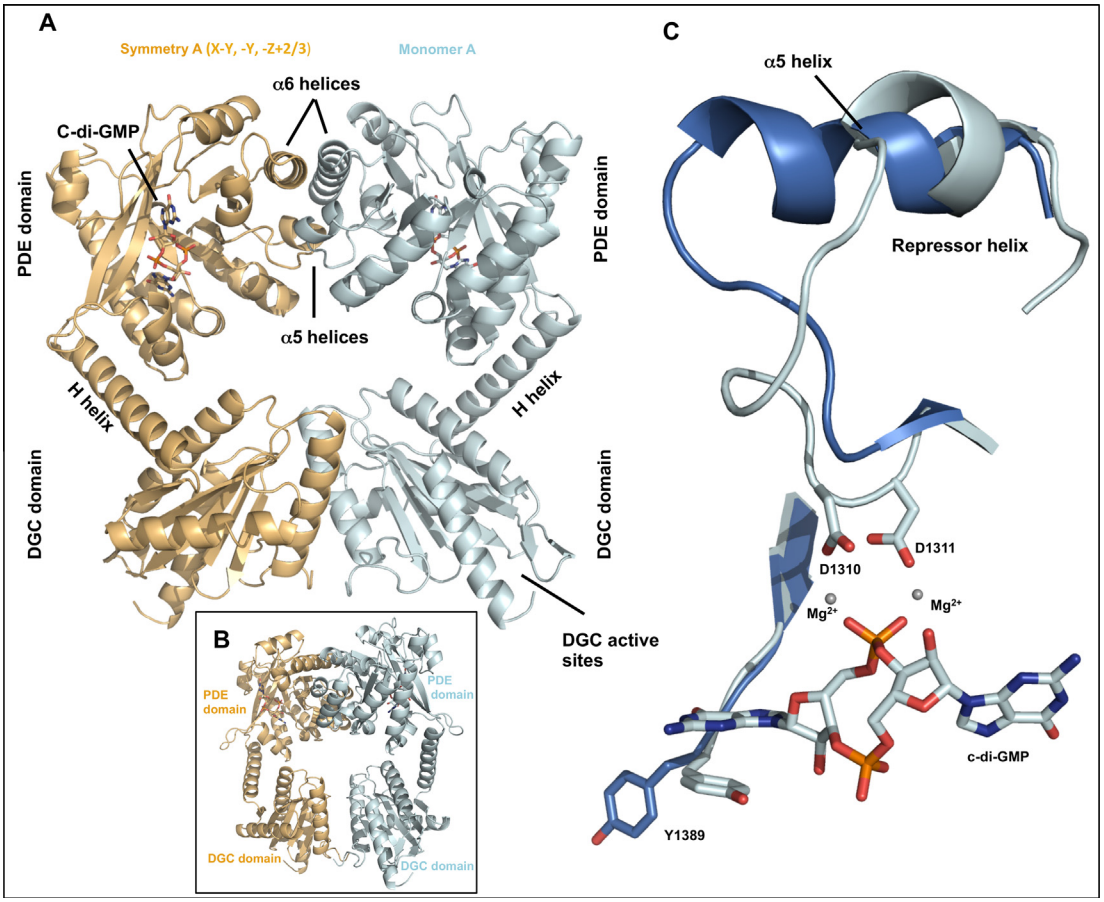

Fig. 3. Crystal structure of the dimeric form of MorA DGC–PDE. (A) Structure of the $DGC–PDE^{978-1409}$ c-di-GMP complex forms a PDE dimer, similar to the isolated $PDE^{1145-1409}$ dimer (Fig. 2 and Table S2). Monomer A is coloured light-blue, the symmetry mate (X–Y, –Y, –Z + 2/3) is shown in light-orange. (B) Fig. 3A rotated by 30°. The DGC domains are not interacting in this dimer. (C) Overlay of the two different PDE states determined: monomeric $PDE^{1144-1409}$ in the nucleotide free repressed state (marine blue) and the nucleotide-bound $DGC–PDE^{978-1409}$ structure in the dimeric state (light-blue). The Repressor helix, PDE-α5, changes in orientation and length, affecting the structure of the catalytic DDFGTG motif. In the repressed state the aspartates of the DDFGTGYSS motif are removed from the active site, in the dimeric state the motif forms an extended loop that allows the residues to engage Mg^{2+} and substrate.

stabilise the DDFGTGYSS motif into an extended loop conformation that allows the aspartates of the DDFGTG motif to bind Mg^{2+} and contribute to active site formation. A further difference is observed with respect to the residue Tyr1389 that acts as a gate to the active site and is involved in base stacking of one of the c-di-GMP guanosine moieties (Figs. 2A and 3C).

When the nucleotide-free DGC–PDE mutant and the nucleotide-bound DGC–PDE structures are compared, a slight rotation of 20° is observed between the DGC and PDE domains (SFig. 4). The rotation suggests that a hinge, located on the H helix (hinge), links the DGC and PDE domains. This hinge is located on the EAL domain side. Other orientations of the two domains might be possible.

4. Conclusion

The tandem DGC–PDE MorA structure represents the first structure determined for a dual active DGC and PDE enzyme. From comparison of the four structures determined, we provide evidence of a conformational change occurring around the R helix (PDE-α5) of the PDE domain that can repress catalytic activity by removing the DDFGTG motif form the active site. We show how the conserved YS residues of the DDFGTGYSS motif are involved in PDE dimerisation to promote structural changes that enable the enzyme to bind c-di-GMP. Dimer interactions favour a shortened R helix and allow the two catalytic aspartates of the DDFGTGYSS motif to enter the active site. Regulation of PDE activity must now be put in the context of protein dimerisation. The challenge is to understand the influence of MorA domains outside the DGC–PDE, such as the transmembrane localisation or the PAS domains. A deciphering of the further regulatory mechanisms within MorA and other tandem DGC–PDE proteins is essential for the development of drugs that tackle biofilm formation and to understand the regulation of bacterial virulence.

Acknowledgements

This work was supported by a grant from the BBSRC. We thank Stuart Findlow and Chris Holes at the Macromolecular Crystallisation Facility, Peter Horton and Simon Coles at the Southampton Diffraction Centre, and Neville Wright at the Biophysics Facility. We thank Tilman Schirmer for the generous gift of the YedH expression clone. We thank staff at the Diamond Light Source and the European Synchrotron Radiation Facility for access and excellent user support.

Appendix A. Supplementary data

Supplementary data associated with this article can be found, in the online version, at http://dx.doi.org/10.1016/j.febslet.2014.11.002.

References

[1] Costerton, J.W., Stewart, P.S. and Greenberg, E.P. (1999) Bacterial biofilms: a common cause of persistent infections. Science 284 (5418), 1318–1322.
[2] Hall-Stoodley, L., Costerton, J.W. and Stoodley, P. (2004) Bacterial biofilms: from the natural environment to infectious diseases. Nat. Rev. Microbiol. 2 (2), 95–108.
[3] Moreau-Marquis, S., Stanton, B. and O'Toole, G. (2008) *Pseudomonas aeruginosa* biofilm formation in the cystic fibrosis airway. Pulm. Pharmacol. Ther. 21 (4), 595–599.
[4] Drenkard, E. and Ausubel, F. (2002) Pseudomonas biofilm formation and antibiotic resistance are linked to phenotypic variation. Nature 416 (6882), 740–743.
[5] Ross, P. et al. (1986) Control of cellulose synthesis *Acetobacter xylinum*. A unique guanyl oligonucleotide is the immediate activator of the cellulose synthase. Carbohydr. Res. 149 (1), 101–117.
[6] Tal, R. et al. (1998) Three cdg operons control cellular turnover of cyclic di-GMP in *Acetobacter xylinum*: genetic organization and occurrence of conserved domains in isoenzymes. J. Bacteriol. 180 (17), 4416–4425.
[7] Ausmees, N. et al. (2001) Genetic data indicate that proteins containing the GGDEF domain possess diguanylate cyclase activity. FEMS Microbiol. Lett. 204 (1), 163–167.
[8] Römling, U., Galperin, M.Y. and Gomelsky, M. (2013) Cyclic di-GMP: the first 25 years of a universal bacterial second messenger. Microbiol. Mol. Biol. Rev. 77 (1), 1–52.
[9] Barraud, N. et al. (2006) Involvement of nitric oxide in biofilm dispersal of *Pseudomonas aeruginosa*. J. Bacteriol. 188 (21), 7344–7353.
[10] Karatan, E. and Watnick, P. (2009) Signals, regulatory networks, and materials that build and break bacterial biofilms. Microbiol. Mol. Biol. Rev. 73 (2), 310–347.
[11] Schmidt, A.J., Ryjenkov, D.A. and Gomelsky, M. (2005) The ubiquitous protein domain EAL is a cyclic diguanylate-specific phosphodiesterase: enzymatically active and inactive EAL domains. J. Bacteriol. 187 (14), 4774–4781.
[12] Aravind, L. and Koonin, E. (1998) The HD domain defines a new superfamily of metal-dependent phosphohydrolases. Trends Biochem. Sci. 23 (12), 469–472.
[13] Bellini, D. et al. (2014) Crystal structure of an HD-GYP domain cyclic-di-GMP phosphodiesterase reveals an enzyme with a novel trinuclear catalytic iron centre. Mol. Microbiol. 91 (1), 26–38.
[14] Rao, F., Yang, Y., Qi, Y. and Liang, Z.-X. (2008) Catalytic mechanism of cyclic di-GMP-specific phosphodiesterase: a study of the EAL domain-containing RocR from *Pseudomonas aeruginosa*. J. Bacteriol. 190 (10), 3622–3631.
[15] Sundriyal, A. et al. (2014) Inherent regulation of EAL domain-catalyzed hydrolysis of second messenger c-di-GMP. J. Biol. Chem. 289 (10), 6978–6990.
[16] Barends, T. et al. (2009) Structure and mechanism of a bacterial light-regulated cyclic nucleotide phosphodiesterase. Nature 459 (7249), 1015–1018.
[17] Navarro, M.V.A.S., De, N., Bae, N., Wang, Q. and Sondermann, H. (2009) Structural analysis of the GGDEF-EAL domain-containing c-di-GMP receptor FimX. Structure 17 (8), 1104–1116.
[18] Kulasakara, H. (2006) Analysis of *Pseudomonas aeruginosa* diguanylate cyclases and phosphodiesterases reveals a role for bis-(3′–5′)-cyclic-GMP in virulence. Proc. Natl. Acad. Sci. 103 (8), 2839–2844.
[19] Navarro, M.V.A.S. et al. (2011) Structural basis for c-di-GMP-mediated inside-out signaling controlling periplasmic proteolysis. PLoS Biol. 9 (2), e1000588.
[20] Choy, W.-K., Zhou, L. and Syn, C.K.-C. (2004) MorA defines a new class of regulators affecting flagellar development and biofilm formation in diverse *Pseudomonas* Species. J. Bacteriol. 186 (21), 7221–7228.
[21] Moglich, A., Ayers, R.A. and Moffat, K. (2009) Structure and signaling mechanism of Per-Arnt-Sim domains. Structure 17 (10), 1282–1294.
[22] Kuchma, S., Connolly, J. and O'Toole, G. (2005) A three-component regulatory system regulates biofilm maturation and type III secretion in *Pseudomonas aeruginosa*. J. Bacteriol. 187 (4), 1441–1454.
[23] Meissner, A. et al. (2007) *Pseudomonas aeruginosa* cupA-encoded fimbriae expression is regulated by a GGDEF and EAL domain-dependent modulation of the intracellular level of cyclic diguanylate. Environ. Microbiol. 9 (10), 2475–2485.
[24] An, S., Je, Wu and Zhang, L.-H. (2010) Modulation of *Pseudomonas aeruginosa* biofilm dispersal by a cyclic-di-GMP phosphodiesterase with a putative hypoxia-sensing domain. Appl. Environ. Microbiol. 76 (24), 8160–8173.
[25] Zähringer, F., Massa, C. and Schirmer, T. (2011) Efficient enzymatic production of the bacterial second messenger c-di-GMP by the diguanylate cyclase YdeH from *E. coli*. Appl. Biochem. Biotechnol. 163 (1), 71–79.
[26] Winn, M.D. et al. (2011) Overview of the CCP4 suite and current developments. Acta Cryst. D 67 (4), 235–242.
[27] Afonine, P.V., Grosse-Kunstleve, R.W. and Adams, P.D. (2005) Phenix refine. CCP4 Newsl, 42.
[28] McCoy, A.J. et al. (2007) Phaser crystallographic software. J. Appl. Cryst. 40 (4), 658–674.
[29] Emsley, P. and Cowtan, K. (2004) Coot: model-building tools for molecular graphics. Acta Crystallogr. D 60 (12), 2126–2132.
[30] Langer, G., Cohen, S., Lamzin, V. and Perrakis, A. (2008) Automated macromolecular model building for X-ray crystallography using ARP/wARP version 7. Nat. Protoc. 3 (7), 1171–1179.
[31] Hayward, S. and Berendsen, H.J.C. (1998) Systematic analysis of domain motions in proteins from conformational change; new results on citrate synthase and T4 lysozyme. Proteins Struct. Funct. Genet. 30 (2), 144–154.
[32] Krissinel, E. and Henrick, K. (2005) Detection of protein assemblies in crystals. Comput. Life Sci., 163–174 (Springer).
[33] A. Kuzin, et al., X-Ray Structure of Protein (EAL/GGDEF domain protein) from *M. capsulatus*, Northeast Structural Genomics Consortium Target McR174C. RCSB PDB (2009).
[34] Tchigvintsev, A. et al. (2010) Structural insight into the mechanism of c-di-GMP hydrolysis by EAL domain phosphodiesterases. J. Mol. Biol. 402 (3), 524–538.
[35] Chan, C. et al. (2004) Structural basis of activity and allosteric control of diguanylate cyclase. Proc. Natl. Acad. Sci. 101 (49), 17084–17089.
[36] Brändén, C.-I. (1991) The TIM barrel—the most frequently occurring folding motif in proteins. Curr. Opin. Struct. Biol. 1 (6), 978–983.
[37] Hou, Y., Li, D.F. and Wang, D.C. (2013) Crystallization and preliminary X-ray analysis of the flagellar motor brake' molecule YcgR with c-di-GMP from *Escherichia coli*. Acta Crystallogr., Sect. F: Struct. Biol. Cryst. Commun. 69 (6), 663–665.
[38] Giardina, G. et al. (2013) Investigating the allosteric regulation of YfiN from *Pseudomonas aeruginosa*: clues from the structure of the catalytic domain. PLoS ONE 8 (11), e81324.